J Therm Anal Calorim (2011) 103:339–345
DOI 10.1007/s10973-010-0948-9

# DSC and morphological studies on the crystallization behavior of $\beta$-nucleated isotactic polypropylene composites filled with Kevlar fibers

**Yewen Cao · Jiachun Feng · Peiyi Wu**

Received: 15 March 2010 / Accepted: 28 June 2010 / Published online: 13 July 2010

**Abstract** The crystallization behavior of $\beta$-nucleated isotactic polypropylene (PP) composites filled with Kevlar fibers (KFs), as well as that of non-nucleated PP/KF composites for comparison, was investigated using differential scanning calorimetry (DSC) and polarized optical microscopy (POM). The morphological observations revealed that the KF addition could induce thick $\alpha$-transcrystalline layer around their surfaces in PP/KF composites, while no obvious transcrystalline layer could be detected in $\beta$-nucleated PP/KF composites. Detailed DSC investigations suggested that for the PP/KF composites, the dominant modification was $\alpha$-form, and the crystallization process of matrix was promoted by KF addition, as illustrated by faster isothermal crystallization rate, shorter induction time, and higher crystallization temperature. However, for $\beta$-nucleated PP/KF composites, the main modification was $\beta$-form, and their crystallization characteristics were independent of KF addition, indicating that the $\alpha$-nucleating effect of KFs was absent in this system. The DSC results were confirmed by further rheological and wide angle X-ray diffraction (WAXD) studies. The mechanism of the formation of transcrystalline layer was also discussed.

**Keywords** DSC · POM · $\beta$-Nucleated isotactic polypropylene · Kevlar fiber · Transcrystalline layer

Y. Cao · J. Feng (✉) · P. Wu
Key Laboratory of Molecular Engineering of Polymers of Ministry of Education, Department of Macromolecular Science and Laboratory of Advanced Materials, Fudan University, Shanghai 200433, People's Republic of China
e-mail: jcfeng@fudan.edu.cn

## Introduction

One of the most important features of polymeric materials is the possibility of controlling their macroscopic physical properties by tailored manipulation of their structure at a microscopic scale. For example, the mechanical properties of semicrystalline polymers are controlled by the aggregation structure of crystalline and amorphous phases or the higher-order structure [1, 2]. On the other hand, the spatial organization and crystallite alignment of semicrystalline polymers are sensitive to the incorporation of other materials, such as reinforcing fibers, elastomers, and nucleating agents [3–5]. Therefore, it provides the possibility to enhance the extrinsic performance of semicrystalline polymers by filler addition.

In composite systems of semicrystalline thermoplastic matrices, a highly oriented crystalline domain, known as the transcrystalline layer, can be developed around the fibers due to the high density of active nuclei on the matrix/fiber interface [6]. During transcrystallization, the extension of the spherulites is laterally hindered by the closely packed nuclei, and forced to grow normal to the fiber surface [7]. Since transcrystalline layer at interfaces is an effective and economical method for improving interfacial adhesion, which could greatly enhance the mechanical properties of the composites, it has attracted numerous attention [6–15]. The nucleation and transcrystalline growth are reported to be system-dependent, that is, affected by the topography of the fiber, the mismatch of thermal expansion coefficients between fiber and matrix, thermal conductivity and surface energy of fiber, chemical composition of fiber surface, and stress-induced crystallization by local flow [9].

In the case of isotactic polypropylene (PP) as the matrix, the transcrystalline morphology is potentially complex because of the polymorphic nature of this polymer. Depending on the polymerization procedure, thermal history and use of different nucleating agents, when crystallized from the melt, the PP chains can organize several spatial arrangements giving rise to different crystalline polymorphs such as α-monoclinic, β-trigonal, and γ-orthorhombic, as well as an intermediate order mesomorphic phase [16–20]. Among these modifications, the α-form is the most common one [16], and the β-form is produced only under special crystallization conditions or in the presence of selective β-nucleating agents (β-NAs) [21–23]. It has been suggested that β-form of PP does not nucleate directly on the fiber surface but grows always on top of a preceding thin α-layer that nucleates initially on the fiber surface [10]. As reported previously, transcrystalline layer with mixed polymorphic content can be formed in PP/fiber composites by coating glass fibers with a specific β-NA [10]. However, in the view of industrial scale, the most effective and accessible way to obtain high level of β-phase is the incorporation of β-NA into matrix. Obtaining high level of β-transcrystallization through the joint addition of fibers and β-NA is faced with a great challenge: the β-nucleating effect of β-NA is always suppressed by fiber introduction [24]. In our previous study, we reported a rare earth β-nucleating agent which could effectively induce the formation of β-modification [25]. Using this β-NA, we have successfully prepared PP/whisker/β-NA composites with β-form as main modification [26]. Moreover, when the whiskers were replaced by Kevlar fibers (KFs), aramid fibers with moderate α-nucleation ability [7], the dominant modification in the composites was also β-form. Since KFs have been extensively reported on their transcrystalline inducement [11, 12], it is of great significance to take systematical characterizations on the crystallization behavior, especially crystalline morphology, of PP/KF/β-NA system.

The aim of this study is to clarify the crystallization behavior, especially crystalline morphology of β-nucleated PP/KF composites, as well as that of non-nucleated PP/KF composites for the sake of comparison. Based on the obtained results, the mechanism of the formation of transcrystalline layer was discussed.

## Experimental

### Materials

The PP used in this study was F401, a product of the Yangzi Petrochemical Co. (Nanjing, China), and it had a melt flow rate (MFR) of 2.5 g 10 $\text{min}^{-1}$ (230 °C, 2.160 kg). The Kevlar fibers chosen were Kevlar 29 fibers (diameter 12–14 μm), provided by Howaytech Co. (Shanghai China). The fibers were washed in acetone and then overdried at 60 °C for 12 h to remove contaminants from the fiber surface prior to mixing. The rare earth-containing β-NA, WBG, was supplied by Guangdong Winner Functional Materials Co. (Foshan, China).

### Sample preparation

The KFs up to 10 wt% loading were melt-compounded with non-nucleated PP and β-nucleated PP using physical mixer. In the β-nucleated PP, the concentration of β-NA was 0.1 wt%, at which this nucleant could effectively promote the formation of β-phase based on our previous study [25]. The ultimate PP/KF (with different KF content of 2.5, 5, 7.5, and 10 wt%) samples are termed as 2.5, 5, 7.5, and 10 K-PP, respectively. Similarly, the PP/KF/β-NA specimens with above KF content are denoted as 2.5, 5, 7.5, and 10 K-BPP, respectively. The neat non-nucleated PP and β-nucleated PP are designated as PP and BPP, which were prepared by the same method for comparison.

### Characterizations and measurements

#### *Polarized optical microscopy (POM)*

Crystalline morphologies of some selected samples were observed using an Olympus BX-51 polarized optical microscope with a Linkam-THMS600 hot stage. The sample films for POM observation were prepared by compression molding at 200 °C. The film specimens sandwiched between two microscope cover slips were first heated to 210 °C and kept there for 5 min to erase any thermal history. Then, they were cooled to the fixed crystallization temperature of 134 °C at a rate of 50 °C $\text{min}^{-1}$ for enough time to isothermally complete the crystallization of PP and the crystalline morphologies were observed. The nitrogen gas was purged through the hot stage during tests.

#### *Differential scanning calorimetry (DSC)*

A DSC 822$^{e}$ thermal analysis system (Mettler Toledo Instruments Inc. Switzerland) with nitrogen as purge (80 ml $\text{min}^{-1}$) was used to investigate the isothermal crystallization kinetics as well as the non-isothermal crystallization behavior of the samples. For DSC measurements, samples (about 8 mg) were placed in an aluminum crucible with a lid crimping onto the pan, and changes in heat flow were measured with respect to an empty aluminum crucible. The non-isothermal crystallization behavior of the specimens was studied by melting the samples at 200 °C for 5 min to erase any thermal history. Subsequently, they were cooled to 100 °C at a cooling rate of 10 °C $\text{min}^{-1}$. The specimens were only cooled to 100 °C in order to suppress the β-to-α recrystallization, as proposed by Varga [27]. Then, the samples were heated to 200 °C again at a heating rate of 10 °C $\mathrm{min}^{-1}$. In the case of isothermal crystallization kinetics, the samples were heat-treated at 200 °C for 5 min in order to eliminate any thermal history. Then, they were cooled at a rate of 50 °C $\mathrm{min}^{-1}$ to the crystallization temperature of 134 °C, and maintained at that temperature during the time for complete crystallization of PP.

### *Advanced rheometric expansion system (ARES)*

The isothermal crystallization kinetics of the specimens was also studied on an ARES Strain-Controlled Dynamic Torsion Rheometer, equipped with TA Orchestrator software. Testing sample disks with a thickness of 1.5 mm and a diameter of 25 mm were prepared by injection molding at 210 °C using a laboratory mixing molder (LMM). The test samples were first heated to 200 °C for 5 min to eliminate the pristine crystalline structures and then cooled rapidly to the desired crystallization temperature of 134 °C at a cooling rate of 30 °C $\mathrm{min}^{-1}$. Finally, the crystalline processes were followed as under small-amplitude oscillatory shear state (strain = 0.1%, frequency = 1 Hz).

### *Wide angle X-ray diffraction (WAXD)*

The crystalline structure was determined by WAXD analysis. The specimens for WAXD were prepared by compression molding into 1-mm-thick sheets at 200 °C. WAXD profiles were recorded on a PANalytical X'pert diffractometer (PANalytical, Netherlands) in the reflection mode with Ni-filtered Cu K$\alpha$ radiation (40 kV, 40 mA). All WAXD data were collected from $2\theta = 8$–28° with a scanning rate of 0.05° $\mathrm{s}^{-1}$.

## Results and discussion

### Crystalline morphology

Figure 1 shows the polarized optical micrographs of different samples crystallized at 134 °C. In contrast to dominant $\alpha$-spherulitic structure in the neat PP (Fig. 1a), oriented $\alpha$-crystalline overgrowth perpendicular to the KF surfaces are observed in the KF reinforced PP (Fig. 1b). This supermolecular structure is identified as the transcrystalline interface [6]. The transcrystalline growth has been studied widely [6–15], and it is commonly agreed that extensive heterogeneous nucleation of polymer melts at high energy surfaces generates transcrystalline layers in the interfacial region [13]. At high heterogeneous nucleation ability of the surface, the extension of the spherulites is laterally hindered by the closely packed nuclei, and forced to grow normal to the fiber surface [7]. As aramid fibers, KFs are gifted with high surface energy and thus moderate $\alpha$-nucleation ability [7], which facilitate the development of $\alpha$-transcrystalline region around them. Moreover, the thickness of $\alpha$-transcrystalline layer is about 50 µm, which is much larger than that of KF diameter.

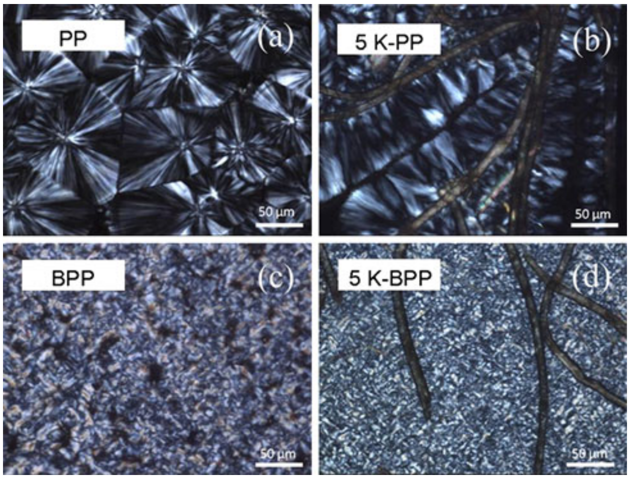

**Fig. 1** The polarized optical micrographs of **a** PP, **b** 5 K-PP, **c** BPP and **d** 5 K-BPP crystallized at 134 °C

However, when $\beta$-NA is introduced into this composite system (Fig. 1d), the crystals in the matrix are composed of small high-birefringent $\beta$-spherulites, with no transcrystalline layer observed in this sample. A number of studies have shown that the essential prerequisite for transcrystallization is the presence of a high density of active nuclei on the fiber surface [6–9]. As suggested by Na et al. the transcrystalline layer is a matter of competition between interface nucleation and bulk nucleation, namely, if interface nucleation is faster than bulk nucleation, transcrystallization will develop. If not, it will be suppressed [6]. Obviously, the disappearance of transcrystalline layer after the introduction of $\beta$-NA indicates that the $\beta$-NA could greatly promote the nucleation process of matrix, making the density of active nuclei in the bulk larger than that on the fiber surface. Therefore, it is unfeasible to induce $\beta$-transcrystallization layer with the combination of $\beta$-NA introduction and filler addition. This statement would be discussed in detail in the following sections. Furthermore, when comparing the crystalline morphology of BPP with that of 5 K-BPP (Fig. 1c, d), we could find that the KF addition has no suppression on the $\beta$-spherulites. In our previous study, this coexistence of fillers and $\beta$-modification has been detected for PP/whiskers/$\beta$-NA system [26].

### Isothermal crystallization

DSC, a conventional and powerful technique to study the crystallization behavior of polymer materials [28, 29], is used in this work. Fig. 2a illustrates the curves of relative crystallinity $X_t$ versus crystallization time $t$ at 134 °C for samples of neat PP, 10 K-PP, BPP, and 10 K-BPP. The relative crystallinity, $X_\mathrm{t}$, is calculated from DSC isothermal crystallization traces (at 134 °C) by integration of the exothermal peaks using the following equation:

$$X_\mathrm{t} = \frac{X_\mathrm{t}(t)}{X_\mathrm{t}(\infty)} = \int_0^t \left(\frac{\mathrm{d}H}{\mathrm{d}t}\right)\mathrm{d}t \Bigg/ \int_0^\infty \left(\frac{\mathrm{d}H}{\mathrm{d}t}\right)\mathrm{d}t \qquad (1)$$

where (d$H$/d$t$) is the rate of heat evolution, $X_t(t)$ and $X_t(\infty)$ represent the absolute crystallinity at time $t$ and at the termination of the crystallization process, respectively. Moreover, since the half crystallization time $t_{1/2}$ (defined as the time required to reach 50% of the complete crystallization) is a very important parameter describing the overall crystallization rate, the relationship between $t_{1/2}$ value at 134 °C and KF loading is illustrated in Fig. 2b. For non-nucleated system, the crystallization rate increases ($t_{1/2}$ decreases) with the increase of KF content. For example, the $t_{1/2}$ of PP is about 16.35 min, and it decreases to 3.70 min for 10 K-PP. It can be concluded that KFs could serve as an α-NA and accelerate the crystallization process of PP. However, compared with β-NA, which can shorten the $t_{1/2}$ from 16.35 min (PP) to 1.55 min (BPP), KFs are obviously much less efficient in accelerating the crystallization of PP. Meanwhile, the introduction of KFs into β-nucleated PP has almost no effect on the crystallization rate of matrix, which is reflected on the constant $t_{1/2}$ within the experimental error for all the β-nucleated samples.

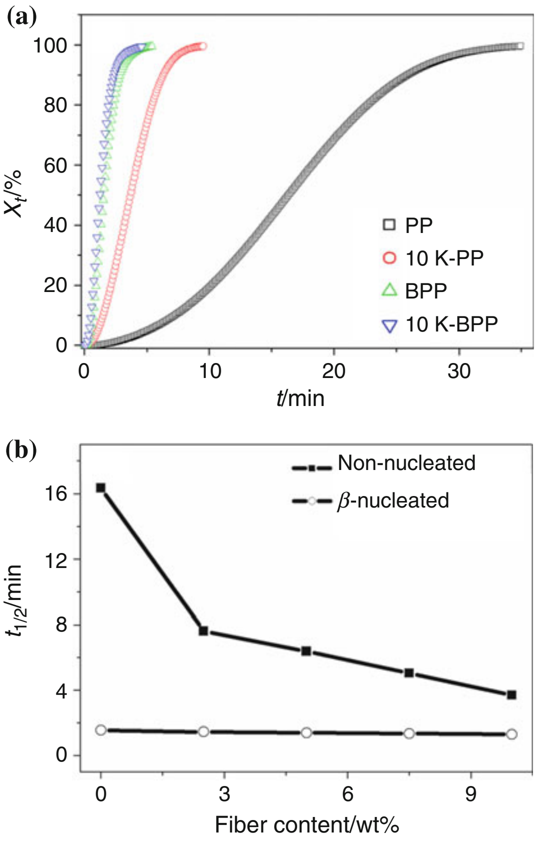

**Fig. 2** **a** Dependence of the relative crystallinity on crystallization time at 134 °C for samples of neat PP, 10 K-PP, BPP and 10 K-BPP, as well as **b** relationship between the $t_{1/2}$ at 134 °C and KF loading for all samples

Recently, ARES has been extensively employed to investigate the crystallization kinetics of polymer materials [30–33]. We, therefore, also used ARES to study the isothermal crystallization processes of PP, 10 K-PP, BPP, and 10 K-BPP, with their plots of storage modulus ($G'$) versus time at 134 °C shown in Fig. 3. For neat PP, before abrupt raise with time, $G'$ initially increases steadily with time, which is referred as the induction stage of nucleation [31]. With the addition 10 wt% KFs, this induction stage is largely shortened, indicating that the nucleation process has been greatly accelerated due to the α-nucleation effect of KFs. Meanwhile, for β-nucleated PP, the induction stage is negligible, and the addition of KFs has no influence on this stage. According to ARES and DSC results which are consistent with each other, the α-nucleation effect of KFs is covered in β-nucleated PP system because the nucleating rate of bulk exceeds that at the fiber surface. The absence of β-transcrystalline layer in this system, as shown in the POM observation, is thus well explained.

## Non-isothermal crystallization

The non-isothermal crystallization process of both non-nucleated and β-nucleated systems was measured by cooling samples from 200 to 100 °C at a standard rate of 10 °C min$^{-1}$ after elimination of thermal history. The DSC cooling curves are presented in Fig. 4. As shown in Fig. 4a for non-nucleated system, the exothermic traces

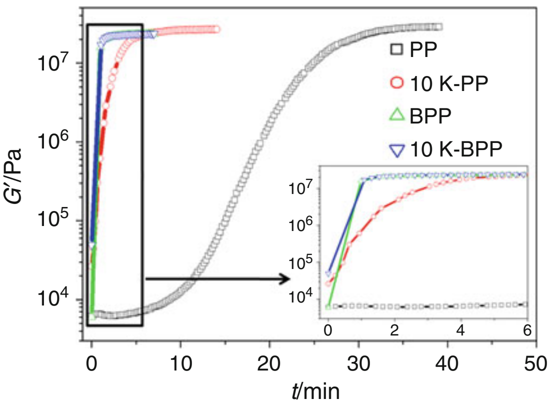

**Fig. 3** Variation of $G'$ with time of neat PP, 10 K-PP, BPP, and 10 K-BPP at 134 °C

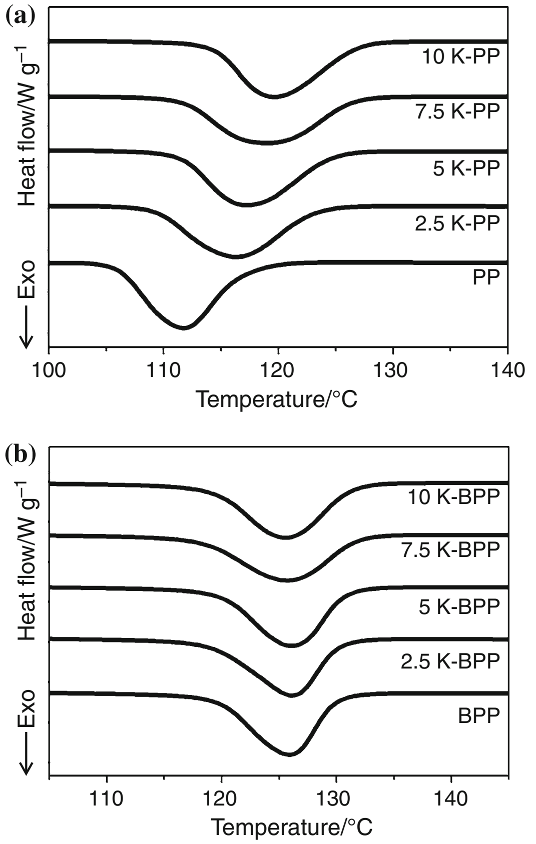

**Fig. 4** DSC thermograms for the crystallization process of **a** non-nucleated and **b** $\beta$-nucleated samples

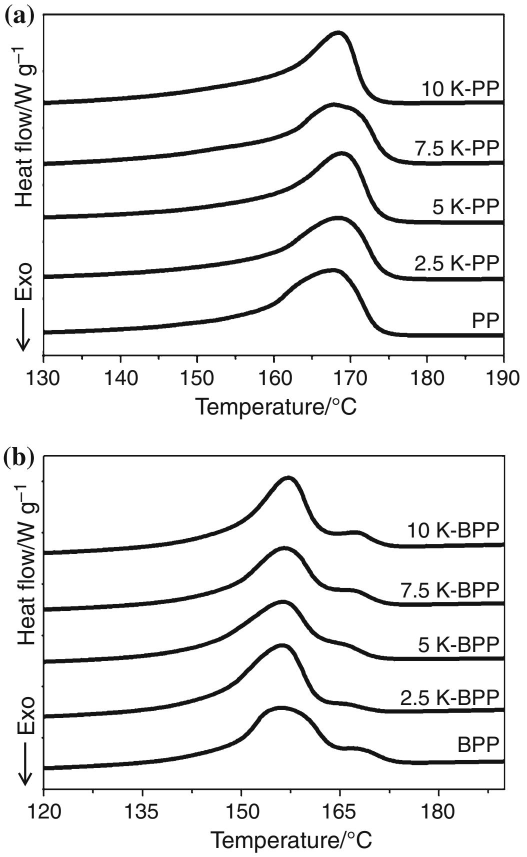

**Fig. 5** DSC thermograms for the melting process of **a** non-nucleated and **b** $\beta$-nucleated samples

shift to higher temperature as a result of KF filling. The improved crystallization temperatures indicate that the KFs alone are efficient in promoting crystallization process of matrix, which is in agreement with the above results. However, it should be noted that the even when the KF loading is up to 10 wt%, the crystallization temperature of 10 K-PP is just about 120 °C, suggesting that the $\alpha$-nucleating effect of KFs is rather limited. In vivid contrast, when 0.1 wt% $\beta$-NA is incorporated into PP, the crystallization temperature of BPP is remarkably raised to more than 125 °C (Fig. 4b). Moreover, the crystallization temperatures for $\beta$-nucleated samples seem to be independent with the KF content, which is another clear evidence of the disappearance of $\alpha$-nucleating effect of KFs in the $\beta$-nucleated system.

In order to investigate the effect of the addition of KFs and $\beta$-NA on the polymorphic content of PP, these non-isothermal crystallized samples were heated to 200 °C at an identical rate of 10 °C min$^{-1}$. Figure 5 demonstrates these DSC heating traces. From Fig. 5a for non-nucleated samples, single melting peak which is almost constant at about 168 °C is observed. However, it is apparent from Fig. 5b that the endothermic curves of $\beta$-nucleated samples exhibit two melting peaks with lower-temperature one absolutely dominant. The endotherm at lower peak temperature of approximately 156 °C could be associated with the melting of the $\beta$-form, while another endotherm approximately located at 168 °C is characteristic for the melting of the $\alpha$-form [26]. These results illustrate that only $\alpha$-modification is formed in the non-nucleated system. In contrast, the $\beta$-nucleated samples crystallize mostly in $\beta$-form, no matter how many KFs are filled. Obviously, the addition of KFs does not have any suppression on the $\beta$-modification of PP, which is consistent with POM observation.

## Crystalline structure

The WAXD patterns of all samples are shown in Fig. 6 to investigate the effect of KFs and $\beta$-NA on the crystalline structure of PP. From Fig. 6a for the WAXD patterns of non-nucleated samples, one can see five most intense WAXD reflections at $2\theta$ angle of 14.0°, 16.8°, 18.6°, 21.2°, and 21.8°, corresponding to the (110), (040), (130), and overlapping (131) and (111) lattice planes of the $\alpha$-monoclinic crystalline structure of PP. Obviously, the addition of KFs does not change the polymorphic content of PP, which is consistent with DSC results. However, it

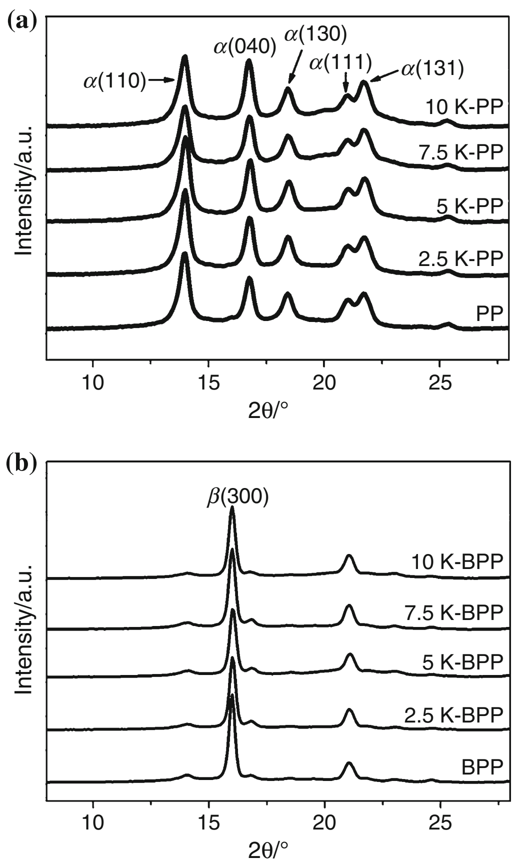

**Fig. 6** WAXD patterns of **a** non-nucleated and **b** β-nucleated samples

should be noted that the relative intensity of diffraction peak at the plane (040) ($2\theta = 14.0^\circ$) increases slightly after fiber addition. Cho et al. ascribed this phenomenon to the preferential orientation of lamellar crystals perpendicular to the fiber surface [13]. In contrast, as shown in Fig. 6b for the WAXD patterns of β-nucleated samples, almost no feature associated with α-form but a peak standing for the (300) diffraction plane of β-trigonal crystalline structure of PP at $2\theta = 16.0^\circ$, is observed. It means that the β-modification is the predominant form in β-nucleated samples and KFs would also not influence the polymorphic content of PP, as an agreement with above results.

## Conclusions

The crystallization behavior, especially crystalline morphology of β-nucleated PP/KF composites, as well as that of non-nucleated PP/KF composites for comparison, was studied using DSC, POM, ARES, and WAXD. The morphological observations revealed that the KF addition could induce thick α-transcrystalline layer around their surfaces in PP/KF composites, while no obvious transcrystalline layer could be detected in PP/KF/β-NA composites. Detailed investigations suggested that KFs could serve as α-NA in PP/KF composites, and the main modification in this system was α-form. However, for PP/KF/β-NA composites, the dominant modification was β-form, and their crystallization characteristics were independent with KF addition, indicating that the α-nucleating effect of KFs was covered by the β-nucleating effect of β-NA. Based on these results, we well explained the absence of transcrystalline layer in PP/KF/β-NA composites: the nucleating rate of β-nucleated PP matrix exceeded that at the fiber surface, and thus the transcrystalline layer was suppressed.

**Acknowledgements** We gratefully acknowledge the financial support from the National Natural Science Foundation of China (Grant No. 20874017, 50673021), the Shanghai-Unilever Research and Development Fund (09520715500), and the National Hi-Tech Research & Development Program (2007AA03Z450).

## References

1. Liang S, Yang H, Wang K, Zhang Q, Du R, Fu Q. Unique crystal morphology and tensile properties of injection-molded bar of LLDPE by adding HDPE with different molecular weights. Acta Mater. 2008;56:50–9.
2. Chen YH, Zhong GJ, Wang Y, Li ZM, Li LB. Unusual tuning of mechanical properties of isotactic polypropylene using counter-action of shear flow and beta-nucleating agent on beta-form nucleation. Macromolecules. 2009;42:4343–8.
3. Zhang MQ, Xu JR, Zhang ZY, Zeng HM, Xiong XD. Effect of transcrystallinity on tensile behaviour of discontinuous carbon fibre reinforced semicrystalline thermoplastic composites. Polymer. 1996;37:5151–8.
4. Muratoglu OK, Argon AS, Cohen RE, Weinberg M. Toughening mechanism of rubber-modified polyamides. Polymer. 1995;36: 921–30.
5. Grein C. Toughness of neat, rubber modified and filled beta-nucleated polypropylene: from fundamentals to applications. Adv Polym Sci. 2005;188:43–104.
6. Na B, Guo M, Yang JH, Tan H, Zhang Q, Fu Q. Crystal morphology and transcrystallization mechanism of isotactic polypropylene induced by fibres: interface nucleation versus bulk nucleation. Polym Int. 2006;55:441–8.
7. Varga J, Karger-Kocsis J. Rules of supermolecular structure formation in sheared isotactic polypropylene melts. J Polym Sci Part B Polym Phys. 1996;34:657–70.
8. Pompe G, Mader E. Experimental detection of a transcrystalline interphase in glass-fibre/polypropylene composites. Compos Sci Technol. 2000;60:2159–67.
9. Dasari A, Yu ZZ, Mai YW. Transcrystalline regions in the vicinity of nanofillers in polyamide-6. Macromolecules. 2007;40: 123–30.
10. Assouline E, Pohl S, Fulchiron R, Gerard JF, Lustiger A, Wagner HD, Marom G. The kinetics of alpha and beta transcrystallization in fibre-reinforced polypropylene. Polymer. 2000;41:7843–54.
11. Klein N, Marom G, Wachtel E. Microstructure of nylon 66 transcrystalline layers in carbon and aramid fibre reinforced composites. Polymer. 1996;37:5493–8.
12. Feldman A, Gonzalez MF, Marom G. Transcrystallinity in surface modified aramid fiber reinforced nylon 66 composites. Macromol Mater Eng. 2003;288:861–6.

13. Cho KW, Kim DW, Yoon S. Effect of substrate surface energy on transcrystalline growth and its effect on interfacial adhesion of semicrystalline polymers. Macromolecules. 2003;36:7652–60.
14. Varga J, Karger-Kocsis J. The occurrence of transcrystallization or row-nucleated cylindritic crystallization as a result of shearing in a glass-fiber-reinforced polypropylene. Compos Sci Technol. 1993;48:191–8.
15. Houshyar S, Shanks RA. Morphology, thermal and mechanical properties of poly(propylene) fibre-matrix composites. Macromol Mater Eng. 2003;288:599–606.
16. Lotz B, Wittmann JC, Lovinger AJ. Structure and morphology of poly(propylenes): a molecular analysis. Polymer. 1996;37: 4979–92.
17. Bruckner S, Meille SV, Petraccone V, Pirozzi B. Polymorphism in isotactic polypropylene. Prog Polym Sci. 1991;16:361–404.
18. Varga J. Crystallization, melting and supermolecular structure of isotactic polypropylene. In: Karger-Kocsis J, editor. Polypropylene: structure, blends and composites, vol. 1. London: Chamman & Hall; 1995. p. 56–115.
19. Krache R, Benavente R, Lopez-Majada JM, Perena JM, Cerrada ML, Perez E. Competition between alpha, beta, and gamma polymorphs in beta-nucleated metallocenic isotactic polypropylene. Macromolecules. 2007;40:6871–8.
20. Menyhard A, Faludi G, Varga J. Beta-crystallisation tendency and structure of polypropylene grafted by maleic anhydride and its blends with isotactic polypropylene. J Therm Anal Calorim. 2008;93:937–45.
21. Varga J. Beta-modification of isotactic polypropylene: preparation, structure, processing, properties, application. J Macromol Sci Phys. 2002;41:1121–71.
22. Shi GY, Zhang XD, Qiu ZX. Crystallization kinetics of beta-phase polypropylene. Makromol Chem. 1992;193:583–91.
23. Varga J, Mudra I, Ehrenstein GW. Highly active thermally stable beta-nucleating agent for isotactic polypropylene. J Appl Polym Sci. 1999;74:2357–68.
24. Mcgenity PM, Hooper JJ, Paynter CD, Riley AM, Nutbeem C, Elton NJ, Adams JM. Nucleation and crystallization of polypropylene by mineral fillers - relationship to impact strength. Polymer. 1992;33:5215–24.
25. Xiao WC, Wu PY, Feng JC, Yao RY. Influence of a novel beta-nucleating agent on the structure, morphology, and nonisothermal crystallization behavior of isotactic polypropylene. J Appl Polym Sci. 2009;111:1076–85.
26. Cao YW, Feng JC, Wu PY. Simultaneously improving the toughness, flexural modulus and thermal performance of isotactic polypropylene by alpha-beta crystalline transition and inorganic whisker reinforcement. Polym Eng Sci. 2010;50:222–31.
27. Varga J. Melting memory effect of the beta-modification of polypropylene. J Therm Anal. 1986;31:165–72.
28. Turi EA. Thermal characterization of polymeric materials. 2nd ed. San Diego: Academic Press; 1997.
29. Varga J. Beta-modification of polypropylene and its two-component systems. J Therm Anal. 1989;35:1891–912.
30. Khanna YP. Rheological mechanism and overview of nucleated crystallization kinetics. Macromolecules. 1993;26:3639–43.
31. Ning NY, Yin QJ, Luo F, Zhang Q, Du R, Fu Q. Crystallization behavior and mechanical properties of polypropylene/halloy site composites. Polymer. 2007;48:7374–84.
32. Acierno S, Pasquino R, Grizzuti N. Rheological techniques for the determination of the crystallization kinetics of a polypropylene-EPR copolymer. J Therm Anal Calorim. 2009;98:639–44.
33. Iervolino R, Somma E, Nobile MR, Chen XM, Hsiao BS. The role of multi-walled carbon nanotubes in shear enhanced crystallization of isotactic poly(1-butene). J Therm Anal Calorim. 2009;98:611–22.